Bioorganic & Medicinal Chemistry 24 (2016) 4108–4119

Contents lists available at ScienceDirect

Bioorganic & Medicinal Chemistry

journal homepage: www.elsevier.com/locate/bmc

Antioxidant, anticancer activities and mechanistic studies of the flavone glycoside diosmin and its oxidovanadium(IV) complex. Interactions with bovine serum albumin

Luciana Naso [a], Valeria R. Martínez [a], Luis Lezama [b,c], Clarisa Salado [d], María Valcarcel [d], Evelina G. Ferrer [a], Patricia A. M. Williams [a,*]

[a] Centro de Química Inorgánica (CEQUINOR, CONICET, UNLP), Departamento de Química, Facultad de Ciencias Exactas, Universidad Nacional de La Plata, Bv. 120 N° 1465 (62 y 63), 1900 La Plata, Argentina
[b] Departamento de Química Inorgánica, Facultad de Ciencia y Tecnología, Universidad del País Vasco UPV/EHU, PO Box 644, 48080 Bilbao, Spain
[c] BCMaterials, Parque científico y Tecnológico de Bizkaia, Edificio 500-1, 48160 Derio, Spain
[d] Innoprot SL, Parque científico y Tecnológico de Bizkaia, Edificio 502-P1, 48160 Derio, Spain

ARTICLE INFO

Article history:
Received 13 May 2016
Revised 22 June 2016
Accepted 26 June 2016
Available online 28 June 2016

Keywords:
Diosmin
Oxidovanadium(IV) complexes
Antioxidant
Anticancer
BSA binding

ABSTRACT

The natural antioxidant flavonoid diosmin, found in citric fruits, showed low antioxidant properties among other flavonoids due to its structural characteristics and low cytotoxicity against lung (A549) and breast (T47D, SKBR3 and MDAMB231) cancer cell lines. The anticancer behavior has been improved by the metal complex generated with the flavonoid and the oxidovanadium(IV) ion. This new complex, $[VO(dios)(OH)_3]Na_5{\cdot}6H_2O$ (VOdios), has been synthesized and characterized both in solid and solution states. The interaction of the metal ion through the sugar moiety of diosmin precluded the improvement of the antioxidant effects. However, the cell-killing effects tested in human lung A549 and breast T47D, SKBR3 and MDAMB231 cancer cell lines, were enhanced by complexation. The anti-proliferative effects on the human lung cancer cell line were accompanied by cellular ROS generation and an increase in cytoplasm condensation. The breast cancer cell lines did not produce caspase3/7 activation, mitochondrial potential reduction and ROS generation. Therefore, a non-apoptotic form of cell death in a caspase- and oxidative stress-independent manner has been proposed. The protein binding ability has been monitored by the quenching of tryptophan emission in the presence of the compounds using bovine serum albumin (BSA) as a model protein. Both compounds could be distributed and transported in vivo and the complex displayed stronger binding affinity and higher contributions to the hydrogen bond and van der Waals forces.

1. Introduction

The genus *Citrus*, one of the most important fruit crops in the world with an annual production exceeding 122.5 million tons in 2010 (FAOSTAT 2012),[1] produces flavanones and flavones in high concentrations, in their free form and/or as glycosides, and lower concentrations of polymethoxyflavones. These compounds are very rare in other plant genera, where they show a species dependent distribution pattern. The degree of expression of these compounds is related to the different stages of cell growth and can be modulated by both chemical (phytoregulators) and physical factors.[2] Recently, more attention had been paid to plant flavonoids and it has been suggested that they might play important roles in anticancer activity.[3] Diosmin (3′,5,7-trihydroxy-4′-methoxyflavone 7-rutinoside) is a flavone glycoside (Fig. 1) found in citric

Abbreviations: AAPH, 2,2-azobis (2- amidinopropane) dihydrochloride; BSA, bovine serum albumin; Crystal violet, Tris(4-(dimethylamino)phenyl)methylium chloride; DMEM, Dulbecco's modified Eagle's medium and; DPPH, 1,1-diphenyl-2-picrylhydrazyl; EDTA, ethylenediaminetetraacetic acid; FBS, fetal bovine serum; DCFH-DA, 2′,7′-dichlorodihydrofluorescein diacetate; 123 DHR, 123 dihydrorhodamine; MMP, mitochondrial membrane potential; MTT, 3-(4,5-dimethylthiazol-2-yl)-2,5diphenyltetrazolium bromide; NADH, reduced nicotinamide adenine dinucleotide; NBT, nitroblue tetrazolium; PMS, phenazinemethosulfate; PBS, phosphate-buffered saline; ROI, regions-of-interest; ROS, reactive oxygen species; RPMI medium, Roswell Park Memorial Institute culture medium; TMRM, tetramethylrhodaminemethylester; VOdios, $[VO(dios)(OH)_3]Na_5{\cdot}6H_2O$.

* Corresponding author.
E-mail address: williams@quimica.unlp.edu.ar (P.A.M. Williams).

http://dx.doi.org/10.1016/j.bmc.2016.06.053
0968-0896/

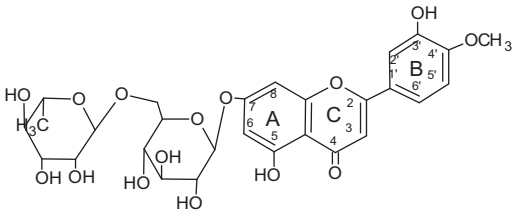

Figure 1. Molecular structure of diosmin.

fruits. As a flavonoid, it possesses a multitude of biological activities including antihyperglycemic, anti-lipid peroxidation, anti-inflammatory, antioxidant, and antimutagenic properties.[4]

Nowadays, diosmin is used in the treatment of venous disease, i.e., chronic venous insufficiency disease, in acute or chronic hemorrhoids, in place of rubber-band ligation, in combination with fiber supplement, or as an adjuvant therapy to hemorrhoidectomy, in order to reduce secondary bleeding.[5] For instance, Daflon 500 mg (Micronized purified flavonoid fraction (MPFF), 450 mg diosmin plus 50 mg hesperidin) produced an increase in venous tone, improves lymph drainage and protects the microcirculation.[6] Diosmin (diosmetin 7-*O*-rutinoside) is structurally related to hesperidin, but it bears a double bond in the C2=C3 position. In a previous communication[7] it has been shown that the oxidovanadium (IV) complex of hesperidin showed superoxide dismutase activity but the antioxidant properties of the flavonoid were not modified by complexation because the metal interacted with the flavonoid through the saccharide moiety. Herein, we have synthesized a new oxidovanadium(IV) complex with diosmin. This compound, $[VO(dios)(OH)_3]Na_5{\cdot}6H_2O$ (VOdios) was characterized by elemental and thermal analyses as well as a series of combined spectroscopic techniques (FTIR, diffuse reflectance, UV–vis, EPR). The ligand and the complex displayed the same antioxidant activities against hydroxyl, superoxide and DPPH· radicals and only improved the capacity to scavenge peroxyl radicals. This behavior has been explained by the lack of interaction of the flavonoid through its rings A and/or C, like in hesperidin. However, the anticancer properties of the ligand (tested in human lung A549 and breast T47D, SKBR3 and MDAMB231 cancer cell lines) have been improved by complexation. Whilst the IC_{50} value on the A549 cell line resulted higher than 100 μM, a strong anticancer effect was observed on the cancer breast cell lines (23.3 μM, 46.4 μM and 11.6 μM, respectively). Activity studies showed different mechanisms of the cell-killing effects of the complex. The interaction of both diosmin and the complex with BSA generates a 1:1 compound protein, by static quenching processes and occurs through H bond and van der Waals interactions.

2. Materials and methods

2.1. Materials

Diosmin (Nanjing Zelang Medical Technology Co., Ltd) and oxidovanadium(IV) chloride (50% aqueous solution, Carlo Erba) were used as supplied. Corning or Falcon provided tissue culture materials. Dulbecco's modified Eagle's medium (DMEM) was purchased from Gibco (Gaithersburg, MD, USA), Tryple™ and fetal bovine serum (FBS) was from GibcoBRL (Life Technologies, Germany). All other chemicals used were of analytical grade. Endotoxin-free RPMI (Roswell Park Memorial Institute) and endotoxin-free Mc Coy media were obtained from Sigma–Aldrich (St Louis, MO). Elemental analysis for carbon and hydrogen was performed using a Carlo Erba EA1108 analyzer. Vanadium content was determined by the tungstophosphovanadic method.[8] Sodium content has been determined by flame photometry. Thermogravimetric analysis was performed with Shimadzu systems (model TG-50), working in an oxygen flow of 50 mL min^{-1} and at a heating rate of 10 °C min^{-1}. Sample quantities ranged between 10 and 20 mg. UV–vis spectra determinations were recorded with a Hewlett–Packard 8453 diode-array spectrophotometer. The diffuse reflectance spectrum was recorded with a Shimadzu UV-300 spectrophotometer, using MgO as a standard. Infrared spectra were measured with a Bruker IFS 66 FTIR spectrophotometer from 4000 to 400 cm^{-1} using the KBr pellet technique. A Bruker ESP300 spectrometer operating at the X-band and equipped with standard Oxford Instruments low-temperature devices (ESR900/ITC4) was used to record the spectrum of the complex at room temperature in the solid state. A computer simulation of the EPR spectra was performed using the program WINEPR SimFonia (version 1.25, Bruker Analytische Messtecnik, 1996). Fluorescence spectra were obtained using a Perkin Elmer (Beaconsfield, UK) LS-50B luminescence spectrometer equipped with a pulsed xenon lamp (half peak height less than 10 μs, 60 Hz), an R928 photomultiplier tube, and a computer working with FLWinlab.

2.2. Synthesis of $[VO(dios)(OH)_3]Na_5{\cdot}6H_2O$ (VOdios)

Diosmin (1 mmol) was dissolved in an aqueous solution (20 mL) by the addition of a concentrated NaOH solution up to pH 12. A 50% aqueous solution of $VOCl_2$ (0.5 mmol) was added with stirring and green solution was formed. Then, a green solid complex was precipitated with isopropyl alcohol. The solid was filtered and washed several times with cold isopropyl alcohol and air-dried. Anal. Calcd for $C_{28}H_{43}O_{25}VNa_5$: C, 35.5; H, 4.5; V, 5.4; Na, 12.2. Exp.: C, 35.3; H, 4.4; V, 5.5; Na, 12.2. UV–vis data for 1:1 $V(IV)O^{2+}$ to diosmin ratio, pH 12, λ_{max} (DMSO): 562 nm and 665 nm. Thermal analysis (TGA) (oxygen atmosphere, 50 mL/min): in the first step (20–200 °C) six water molecules are lost (11.4%). The dehydrated product rendered Na_3VO_4 (characterized by infrared spectroscopy) and Na_2O at 800 °C. The weight of the final residue was 26.0%, in agreement with the theoretical value. Diffuse reflectance spectrum: 700 nm.

2.3. Spectrophotometric titrations and stability studies

In order to establish the stoichiometry of the complex the molar ratio method was applied. An aqueous solution of diosmin (4×10^{-5} M) was prepared and its electronic spectrum recorded. The absorption spectra of different aqueous solutions of 4×10^{-5} M diosmin and $VOCl_2$ in ligand-to-metal molar ratios from 10 to 0.5 (pH 12) were measured. Stability studies have been performed measuring the variation of the VOdios electronic absorption spectra, in DMSO with time, under nitrogen atmosphere.

2.4. Antioxidant properties

2.4.1. Superoxide dismutase assay

The superoxide dismutase (SOD) activity was examined indirectly using the nitroblue tetrazolium (NBT) assay. The indirect determination of the activity of diosmin and VOdios was assayed by their ability to inhibit the reduction of NBT by the superoxide anion generated by the phenazine methosulfate (PMS) and reduced nicotinamide adenine dinucleotide (NADH) system. As the reaction proceeded, the formazan color developed and a change from yellow to blue was observed which was associated with an increase of the intensity of the band at 560 nm in the absorption spectrum. The system contained 0.5 mL of sample, 0.5 mL of 1.40 mM NADH and 0.5 mL of 300 μM NBT, in 0.1 M KH_2PO_4–NaOH buffer (pH 7.5). After incubation at 25 °C for 15 min, the reaction was started by

adding 0.5 mL of 120 μM PMS.[9] Then, the reaction mixture was incubated for 5 min. Each experiment was performed in triplicate and at least three independent experiments were performed in each case. The amount of diosmin or VOdios that gave a 50% inhibition (IC_{50}) was obtained by plotting the percentage of inhibition versus the negative log of the concentration of the tested solution.

2.4.2. 1,1-Diphenyl-2-picrylhydrazyl assay

The antiradical activity of diosmin and VOdios was measured in triplicate using a modified method of Yamaguchi et al.[10] A methanolic solution of 1,1-diphenyl-2-picrylhydrazyl radical ($DPPH^{\cdot}$) (4 mL, 40 ppm) was added to 1 mL of the antioxidant solutions in 0.1 M tris(hydroxymethyl)aminomethane–HCl buffer (pH 7.1) at 25 °C, giving a final concentration of 10 μM. After 60 min of the reaction in the dark, the absorbance at 517 nm was measured and compared with the absorbance of the control prepared in a similar way without the addition of the compounds (this value was assigned arbitrarily as 100%).

2.4.3. Scavenging of the hydroxyl radical

Hydroxyl radicals were generated by the ascorbate–iron–H_2O_2 system. Briefly, the reaction mixture contained 3.75 mM 2-deoxyribose, 2.0 mM H_2O_2, 100 μM $FeCl_3$, and 100 μM EDTA with or without the tested compounds in 20 mM KH_2PO_4–KOH buffer, pH 7.4. The reaction was triggered by the addition of 100 μM ascorbate and the mixture was incubated at 37 °C for 30 min. Solutions of $FeCl_3$, ascorbate, and H_2O_2 were made up in deaerated water immediately before use. The extent of deoxyribose degradation by hydroxyl radical was measured with the thiobarbituric acid method.[11]

2.4.4. Inhibition of peroxyl radical

Peroxyl radicals were generated by the thermal decomposition of 2,2-azobis (2-amidinopropane)dihydrochloride (AAPH).[12] AAPH was chosen due to its ability to generate free radicals at a steady rate for extended periods of time (half-life of 175 h). The consumption of pyranine was followed spectrophotometrically by the decrease in absorbance at 454 nm with a thermostated cell at 37 °C. The reaction solutions contained AAPH (50 mM), pyranine (50 μM) and several concentrations of the tested compounds. The delay of pyranine consumption (lag phase) was calculated as the time before the consumption of pyranine started (notable reductions in absorbance).[13]

2.5. Biological assays

2.5.1. Cell culture

A549 human lung cancer cell line was obtained from ABAC (Argentinean Cell Bank Association INEVH, Pergamino, Buenos Aires, Argentina). DMEM supplemented with 100 U mL^{-1} penicillin, 100 μg mL^{-1} streptomycin and 10% (v/v) fetal bovine serum was used as the culture medium. When 70–80% confluence was reached, cells were sub-cultured using TrypLE™ from Gibco (Gaithersburg, MD, USA), free phosphate buffered saline (PBS) (11 mM KH_2PO_4, 26 mM, Na_2HPO_4, 115 mM NaCl, pH 7.4. Human T47D, MDAMD231 and SKBR3 breast cancer cell lines were obtained from HPA Culture Collection (Salisbury, United Kingdom). The T47D and MDAMD231, cell lines were cultured in endotoxin-free RPMI medium supplemented with 10% FBS, and 100 U/mL penicillin and 100 μg/mL streptomycin. SKBR3 cells were cultured in endotoxin-free Mc Coy medium supplemented with 10% FBS and 100 U/mL penicillin and 100 μg/mL streptomycin. All reagents were from Sigma–Aldrich (St Louis, MO). Cultures were maintained at 37 °C in a humidified atmosphere with 5% CO_2 and passaged according to manufacturer's instructions.

2.5.2. Crystal violet assay. Lung cancer cell line

The compounds were dissolved in DMSO just before the experiment and a calculated amount of these solutions was added to the growth medium containing cells at a final DMSO concentration of 0.5% which had no discernible effect on cell-killing. The growth inhibitory effect towards the cancer A549 cell line was evaluated by means of the crystal violet bioassay. Briefly, 2.0×10^4 cells/well were seeded in 48-well microplates in growth medium (500 μL) and then incubated at 37 °C in a 5% carbon dioxide atmosphere. After 24 h, the medium was removed and replaced with a fresh one containing the compounds to be studied at the appropriate concentration. Triplicate cultures were established for each treatment. After 24 h, each well was stained with crystal violet and washed to remove the excess of dye. The crystal violet taken up by the cells was extracted with the buffer and the inhibition of cell growth induced by the tested compounds was detected by the experimental absorbance obtained for each well at 540 nm. Mean absorbance for each drug dose was expressed as a percentage of absorbance of the control untreated well and the data has been plotted versus drug concentration.

2.5.2.1. Intracellular reactive oxygen species (ROS) generation. ROS generation in the A549 cell line was measured by oxidation of dihydrorhodamine123 (DHR) to rhodamine 123. Cells were incubated during 30 min at 37 °C in 1.5 mL of PBS buffer alone (control condition) or with the compounds in the presence of 10 mM DHR. Media were separated and the cell monolayers rinsed with PBS and lysated into 1 mL 0.1% Triton-X100. The cell extracts were then analyzed for the oxidized product rhodamine by fluorescence spectroscopy (excitation wavelength, 500 nm; emission wavelength, 536 nm), using a Perkin–Elmer LS 50B spectrofluorometer. Results were corrected for protein content, which was assessed by the method of Bradford.[14]

2.5.2.2. Morphological changes. In order to evaluate the morphology of the A549 cell line, cells were grown in six well/-plates and incubated overnight with fresh serum-free DMEM plus 0 (control), 10 and 100 μM solutions of the complex. The monolayers were subsequently washed twice with PBS, fixed with methanol and stained with 1:10 dilution of Giemsa for 10 min. Next, they were washed with water and the morphological changes were examined by light microscopy.

2.5.3. MTT assay. Breast cancer cell lines

Stock complex solutions of compounds were prepared in DMSO with a manipulation time of 15 min. Breast cancer cells were seeded at a density of 5000 cells/well in 96 well plates, grown overnight and treated with either vehicle (DMSO), diosmin, VOdios and oxidovanadium(IV) in DMSO at different concentrations in FBS free medium(Sigma–Aldrich, St. Louis, MO). The dissolution vehicle yield a maximum final concentration of 0.5% in the treated well. After 24 h of incubation, 3-(4,5-methyl-thiazol-2-yl)-2,5diphenyl tetrazolium bromide (MTT) was added at 100 μg/well for 2 h (Sigma–Aldrich, St. Louis, MO).The formazan products generated by cellular reduction of MTT were dissolved in DMSO and the optical density was measured at 450 nm using Sinergy 2 Multi Mode Microplater reader Biotek (Wisnooski, USA). All experiments were done in triplicate. Data were presented as proportional viability (%) comparing the treated group with the untreated cells, for which the viability has been assumed to be 100%.

2.5.3.1. Mechanistic determinations. For the high content analysis image assay the cancer cells were seeded at a density of 5000 cells/well in a collagen-coated 96 well plate and stained with fluorescent probes (Invitrogen, Life Technologies, Madrid, Spain) during 30 min: tetramethyl rhodamine methyl ester (TMRM)

50 μM for the measurement of mitochondrial depolarization related to cytosolic Ca^{2+} transients, 5-(and-6)-chloromethyl-2,7, dichlorodihydrofluorescein diacetate acetyl ester (CMH2DCFDA) 1 μM for the determination of reactive oxygen species production (ROS) and CellEventTM Caspase 3/7 Green Detection Reagent 5 μM for the assessment of caspase 3/7 activation. After 30 min cells were treated with 10 μM concentration of diosmin, VOdios and oxidovanadium(IV) cation during 24 h. The excitation/emission filters for each probe were: 488/10 nm and 515 LP nm (ROS), 555/28 nm and 647/78 nm (TMRM), 488/10 nm and 515 LP nm (CellEvent™ Caspase 3/7 Green Detection Reagent). Using specific AttoVision (BD) software algorithms, the mean intensity of each Region of Interest (ROI) was analyzed. The results are expressed as the mean ± the standard error of the mean. Statistical differences were analyzed using the analysis of variance method (ANOVA) followed by the test of least significant difference (Fisher).

2.6. Bovine serum albumin (BSA) interaction

BSA was dissolved in Tris–HCl (0.1 M, pH 7.4) buffer to attain a final concentration of 6 μM. Diosmin and the complex were added dropwise to the BSA solution and left to rest to ensure the formation of homogeneous solutions with concentrations ranging from 5 to 100 μM. The fluorescence intensity was measured (excitation at 280 nm and emission at 350 nm) at 25, 30 and 37 °C, incubation time 1 h. For each sample and concentration, three independent replicates were performed. The measurements were carried out on a Perkin–Elmer LS-50B luminescence spectrometer (Beaconsfield, England) equipped with a pulsed xenon lamp (half peak height <10 ls, 60 Hz), an R928 photomultiplier tube and a computer working with FLWinLab software. Both excitation and emission slits were set at 10 nm throughout this study.

3. Results and discussion

3.1. Solid characterization of the complex

3.1.1. Vibrational spectroscopy

In order to study the binding mode of diosmin with the oxidovanadium(IV) cation, the FTIR spectra of both the ligand and the complex have been compared. The proposed assignments presented in Table 1 are based on general references.[15,16] The vibrational spectrum of diosmin resembles that of hesperidin.[17] The structural differences between both flavonoids arise because of the presence of the C2=C3 double bond in the former compound. The characteristic C=C (aromatic) absorption band is located at the same position in both cases (1609 cm^{-1}) but it is the most intense vibrational band in the spectrum of diosmin. The other C=C stretching band is red shifted in the diosmin spectrum (1519 cm^{-1} to 1503 cm^{-1}) and it also strengthens its intensity. The carbonyl absorption band assigned to the aromatic ketonic carbonyl stretching (C=O vibration) shifted from 1660 cm^{-1} (diosmin) to 1649 cm^{-1} (very strong, hesperidin), indicating a lower bond order in the latter flavonoid due to the lack of resonance with ring C. Besides, the OH stretching bands at 3466 cm^{-1} and 3413 cm^{-1} shifted ca. 10 cm^{-1} to the blue in hesperidin. The C=O stretching band of diosmin at 1660 cm^{-1} remained unchanged in the VOdios complex although its intensity was reduced, indicating that the carbonyl group was not involved in the complex formation. Besides, a new band appeared at 1633 cm^{-1} and this band is also present in the potassium salt of diosmin (prepared by the addition of a KOH aqueous solution to an aqueous solution of diosmin up to a pH value of 12 followed by the precipitation of the salt with absolute EtOH). For this reason, the interaction of the oxidovanadium(IV) cation with the C=O group has been discarded. The band of the C—O—C stretching mode (ring C) at 1262 cm^{-1} remained unchanged after complexation indicating that this group did not participate of the coordination with the metal center. The bands assigned to C—OH stretchings and deformations shifted and changed their intensities upon complexation. These data together with the strong alkaline media used in the preparation of the complex could indicate that the OH sugar groups of the terminal saccharide ramnose may desprotonate or coordinate by metal interaction. Most of the oxidovanadium(IV) complexes with flavonoids showed ν(V=O) stretching vibrational band at ca. 980 cm^{-1} suggesting that the $V(IV)O^{2+}$ coordination occurs through the O carbonyl atom and the 3-OH or 5-OH groups of the ligand after deprotonation.[18–22] In the VOdios complex, the ν(V=O) stretching vibration band has been observed at relatively low frequencies (921 cm^{-1}) which is an indication that the coordination of oxidovanadium(IV) cation occurred with the formation of a five membered chelate ring through deprotonated pairs of OH groups in the *cis*-position. This type of chelation has previously been observed in oxidovanadium(IV) complexes of mono- and disaccharides[23–25] and other VO–flavonoid complexes.[7,26] In this latter case the coordination takes place through *cis*- aryl-O^- or *cis*-alkyl-O^- groups.

Table 1
Assignment of the main bands of the infrared spectra of diosmin and its oxidovanadium(IV)complex, VOdios (band positions in reciprocal centimeters)

Diosmin	VOdios	Assignments
3468br	3403 br	$\nu(O—H)_{water}$
3411 br	3201 br	$\nu(O—H)_{phenol}$
2930 m	2927 w	ν(C—H)
2923 br	2924 sh	ν(C—H)
1660 vs	1660 sh	ν(C=O)
1609 vs	1592 m	ν(C=C), ν(C2=C3)
1503 vs	1494 w	ν(C=C), ring C
1448 s	1439 s,br	$\delta(CH_2)$
1413 sh	1413 sh	
1361 m	1349 m	δ(COH)
1315 m	1308 sh	ν(C—OH)
1262 s	1262 s	ν(C—O—C), ν(C—OH)
1205 sh	1209 w	$\delta(CH_2)$
1138 m	1139 m	ν(C—O), δ(C—H arom)
1099 sh	1099 sh	$\nu(C—O)_{endo}$
1067 m	1068 m	$\nu(C—O)_{exo}$
1030 sh	1044 sh	
978 w	978 w	
	921 w	ν(V=O)

Relative intensities of the bands: vs: very strong, s: strong, m: medium, w: weak, vw: very weak, sh: shoulder, br: broad.

3.1.2. Electron paramagnetic resonance (EPR spectroscopy)

The X-band EPR spectrum of the oxidovanadium(IV)–diosmin complex has been recorded at room temperature in the solid state (Fig. 2). The experimental spin Hamiltonian parameters were determined as $g_{II} = 1.958$ and $g_{\perp} = 1.977$ and the hyperfine coupling constants were $A_{II} = 150 \times 10^{-4}$ cm^{-1} and $A_{\perp}$ 48 $\times 10^{-4}$ cm^{-1}. The following empirical relationship described by Chasteen,[27] is frequently used to determine the identity of the equatorial ligands in oxidovanadium(IV) complexes: $A_z = \Sigma \cdot n_i \cdot A_{z,i}$, ($n_i$: number of equatorial ligands of type i, $A_{z,i}$: contribution to the parallel hyperfine coupling from each of them). The calculation of the A_{II} hyperfine coupling constant was performed because it is sensitive to the type of donor atoms on the equatorial positions of the coordination sphere. Considering the contribution to the A values of RO^- = 35.3 $\times 10^{-4}$ cm^{-1} and OH^- = 38.7 $\times 10^{-4}$ cm^{-1} for each potential donor group, the calculated A value for the donor sets in a possible equatorial $VO(RO)_2(OH)_2$ coordination mode in the complex was 148 $\times 10^{-4}$ cm^{-1}.[28] This value corresponded well to the experimental one and then, we can conclude that the binding mode of

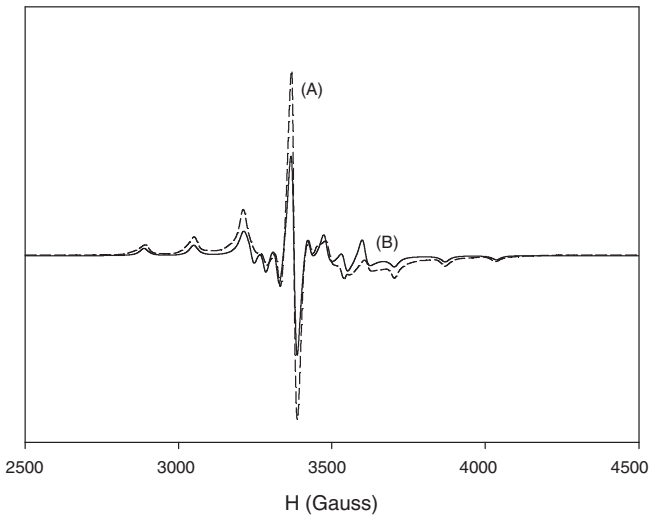

Figure 2. Experimental (A, dotted dash line, room temperature) and calculated (B, solid line) EPR spectrum of the complex $[VO(dios)(OH)_3]Na_5{\cdot}6H_2O$ measured at the X band.

the oxidovanadium(IV) center in this complex could be expected to involve an equatorial coordination sphere with two deprotonated *cis*-OH groups from the sugar moiety and two hydroxyl OH^- anions in the equatorial coordination sphere.

3.2. Solution studies

3.2.1. UV–vis spectra and spectrophotometric titrations

The electronic spectrum of diosmin was recorded in water (pH 12, using NaOH) under a nitrogen atmosphere. The absorption spectrum of diosmin is characterized by two main absorption bands commonly referred to as Band I and Band II. Band I is associated with the absorption of the cinnamoyl system (B + C ring) while Band II with the absorption of the benzoyl moiety formed by the conjugated system of ring A and ring C. Diosmin has several ionizable hydroxyl groups with pK_a values relatively close each other. It can be seen in Figure 3 that the spectral changes occurred at pH values above 9, in agreement with the reported protonation constants of buffered solutions of diosmin dissolved in a minimum quantity of DMSO ($pK_1 = 8.6 \pm 0.2$ and $pK_2 = 10.5 \pm 0.3$).[29]

It can be seen in Figure 4 that diosmin displayed two bands at 269 nm and 372 nm and a shoulder at 298 nm. After formation of complex, the band related with B ring (372 nm) remained unchanged suggesting that this moiety is not involved in the coordination with the metal. The band and the shoulder at lower wavelength occurred at the same energy and increased their intensities indicating that the flavonoid moiety did not interact with the metal center. With the aim to confirm the stoichiometry of the complex VOdios, spectrophotometric titrations were performed (pH 12). The band at 270 nm increased its intensity upon the addition of different quantities of oxidovanadium(IV) (Fig. 5) and the formation of a 1:1 diosmin/$V(IV)O^{2+}$ complex (similar to the silver–diosmin complex)[30] can be determined (inset, Fig. 5).

3.2.2. EPR spectroscopy

In order to identify the solution species present at pH 12, the EPR spectrum of VOdios has been measured in frozen solution using water as solvent (DMSO 5%, pH = 12) (data not shown). The EPR signal indicated the formation of single mononuclear species. The experimental spin Hamiltonian parameters were determined as $g_{II} = 1.961$ and $g_{\perp} = 1.979$ and the hyperfine coupling constants were $A_{II} = 151.8 \times 10^{-4}\,cm^{-1}$ and $A_{\perp}$ $47 \times 10^{-4}\,cm^{-1}$ being these values similar to those found for the solid VOdios complex. Therefore, it could be suggested that the equatorial coordination sphere of oxidovanadium(IV) cation in solution retain the same arrangement (two deprotonated *cis*-OH groups from the sugar moiety and two hydroxyl OH^- anions) than in the solid phase.

3.3. Antioxidant properties

The antioxidant activity of flavonoids depends upon arrangement of functional groups about the nuclear structure. The main structural features of flavonoids required for a good radical scavenging power could be summarized as *ortho*-dihydroxy structure in B ring, 2,3-double bond in conjugation with 4-oxo function in C ring and the presence of hydroxyl groups at positions 3- and 5-.[31] The glycosylation of flavonoids reduce their in vitro antioxidant activity when compared to the corresponding aglycons. The presence of disaccharide rutinose at C-7 on the A ring and the absence of hydroxyl group at C-3 on the B ring makes diosmin a poor antioxidant agent. Like methylation, O-glycosylation interferes with the coplanarity of the B-ring with the rest of the flavonoid and the ability to delocalize electrons.[31] The antioxidant capacity

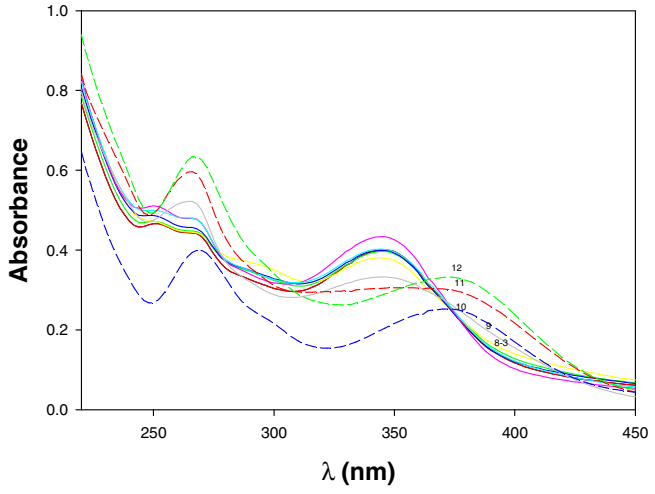

Figure 3. Representative UV–vis absorption spectra of diosmin (4×10^{-5} M) at different pH values.

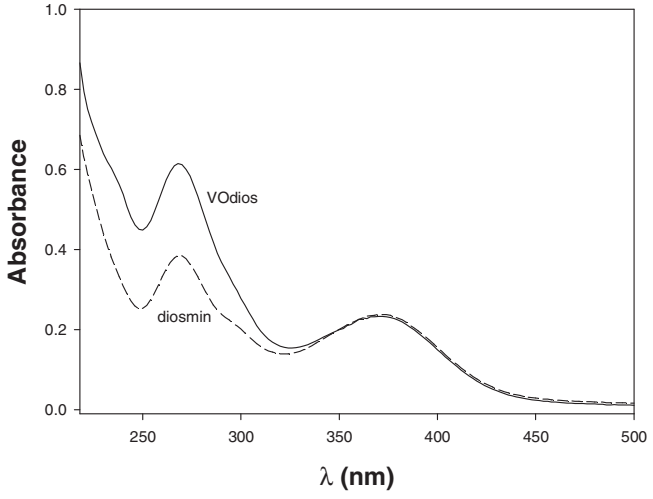

Figure 4. UV–vis spectra of the ligand diosmin and its complex with oxidovanadium(IV) cation in water at pH 12.

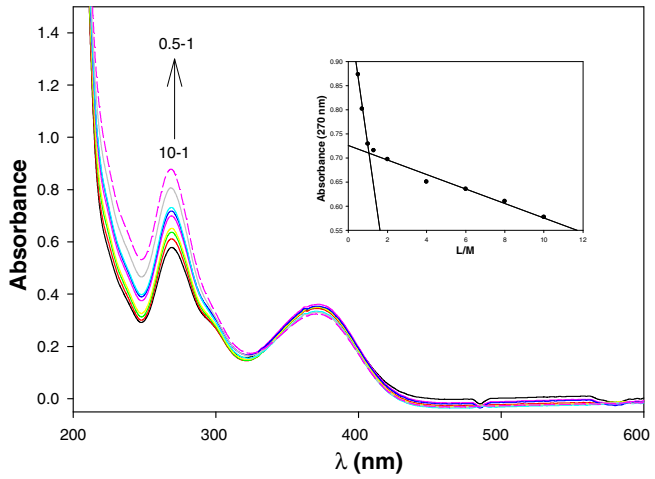

Figure 5. UV–vis spectra of diosmin (4×10^{-5} M) and $VOCl_2$ in ligand-to-metal ratios (L/M) from 10.0 to 0.5 (pH 12). The arrow indicates increasing metal additions. Inset: spectrophotometric determination of the stoichiometry of the VOdios complex at 270 nm by the molar ratio method.

of the oxidovanadium(IV) cation, diosmin and VOdios complex has been measured against the $O_2^{\cdot-}$, DPHH·, OH· and ROO· radicals. In agreement with the particular structure of the complex an enhancement of these properties is not expected.

Figure 6 illustrates the superoxide radical scavenging of diosmin and VOdios. It can be seen that the flavonoid has no capacity to dismutate the superoxide anion in agreement with previous results[32] although other authors found that diosmin scavenges this anion radical in a dose response manner.[33] VOdios behaved as the ligand at low concentrations but it is slightly effective at 100 μM concentration. The oxidovanadium(IV) cation behaved as a good scavenger agent with IC_{50} value 15 μM (IC_{50} for the native enzyme, 0.21 μM).[19]

DPPH assay is considered a valid and easy assay to evaluate the structure–activity relationship (SAR) of antioxidants. This assay is based on the measurement of the scavenging ability of antioxidant compounds towards the stable radical 2,2-diphenyl-1-picrylhydrazyl (DPPH·). The free radical DPPH· (λ_m, 517 nm) is reduced to the corresponding hydrazine when it reacts with hydrogen donors. In agreement with the literature reports it can be seen in Figure 7 that diosmin is not active against DPPH· radical.[34–36] Both the ligand and the VOdios complex behaved as poor antioxidants against DPPH radical (Table 2 and Fig. 7) scavenging only about 15% of DPPH· radical at 100 μM. On the other hand, oxidovanadium(IV) cation acted as a good antioxidant (scavenging about 40% of DPPH· radical at 100 μM).

Although there are discrepancies in literature for the scavenging capacity of diosmin against hydroxyl radical we found a low antioxidant behavior of the flavonoid for this radical (Fig. 8 and Table 2).[33,37] The complexation slightly improved the action of the free ligand at high concentrations.

Pyranine is a spectrophotometric probe that scavenges free radicals, including peroxyl radicals (ROO·). The reduction in pyranine intensity is followed to monitor its interaction with peroxyl radicals at 454 nm. Pyranine declines at a constant rate with minimum delay (lag) following the addition of AAPH. Figure 9 and Table 2 show that VOdios behaved as better peroxyl scavenger than the free ligand.

The structural modification of diosmin by metal complexation produced an improvement of the antioxidant capacity only against peroxyl radicals. This behavior is associated to the coordination mode of the flavonoid and is in concordance with previous determinations.[26] When the metal center bind the flavonoid through the OH groups in *cis*-position on ring B or with a distant substituent of rings B or C (hesperidin, luteolin, diosmin) the phenyl radical generated on the flavonoid by electron or H donation from the different radicals could not be stabilized by the resonance of the π system of the VO cation with the whole aromatic ring.

3.4. Biological assays

3.4.1. In vitro cell cytotoxicity

In a first step, the stability of the complex in DMSO under nitrogen atmosphere has been measured following the variations of the UV–vis spectra with time. No observable variation has been detected at least during 20 min (data not shown). Therefore, it

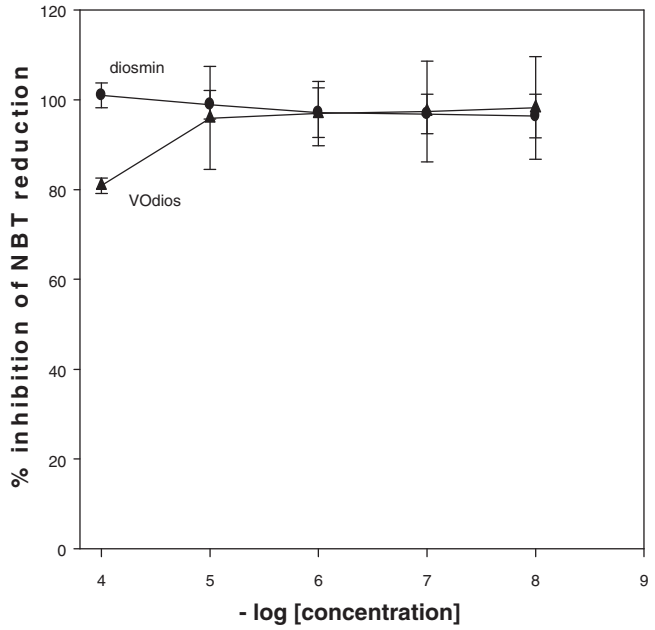

Figure 6. Effects of diosmin and VOdios on the reduction of nitroblue tetrazolium by the generated superoxide radical at 560 nm. The values are expressed as the mean ± SEM of at least three independent experiments.

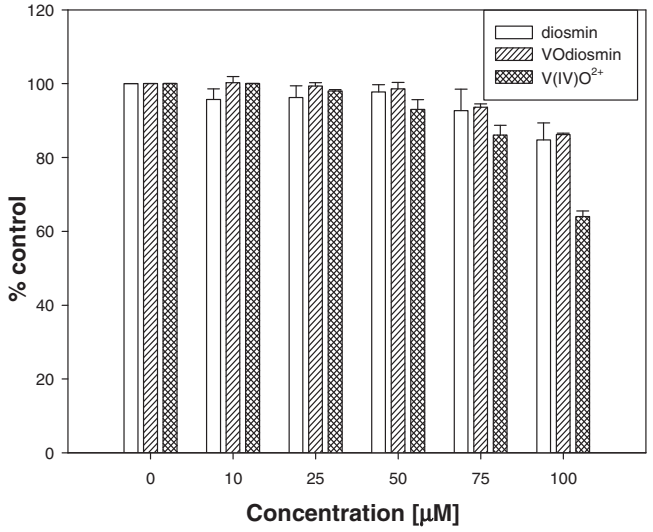

Figure 7. Effects of $V(IV)O^{2+}$ cation, diosmin and VOdios on the reduction in the concentration of DPPH· radical. Values are expressed as the mean ± SEM of at least three independent experiments.

Table 2
Percentage of free radical scavenging of diosmin, VOdios and oxidovanadium(IV). Values are expressed as the mean ± standard error of at least three independent experiments

	Diosmin	VOdios	$V(IV)O^{2+}$
SOD (IC_{50}, μM)	N.A	>100	15[a]
DPPH·, 100 μM % scavenging	14 ± 1	15 ± 5	37 ± 2
OH·, 100 μM % scavenging	N.A	13 ± 4	38 ± 2
ROO·, 100 μM lag phase(min)	1.4	3.0	6.4[b]

N.A not active.
[a] Ref. 19.
[b] Ref. 22.

can be considered that the decomposition of the complex resulted insignificant during the manipulation time of the samples.

3.4.2. Lung cancer cell lines

For flavonoid glycosides, the absence of antiproliferative activities on several human cancer cell lines has in general been observed probably because the sugar moiety can reduce the cytotoxic activity of the corresponding aglycon species.[38,39] It has been suggested that the hydrophilic nature of sugars or the increased volume of glycosides could interfere with the drug entering through the cellular membrane.[40] On the other hand, the in vivo assays showed that diosmin inhibited the hepatocellular tumor growth in a mice model[41] and reduced pulmonary metastasis, both at the macroscopic and microscopic levels.[42]

The effects of the compounds on the A549 cell viability were estimated through the crystal violet assay. As shown in Figure 10, A549 cells treated with diosmin and oxidovanadium(IV) cation showed no anticancer effect at least up to 100 μM concentration and the ANOVA analysis showed that this effect was not found to be significantly different (*p*-value, 0.05). However, for an incubation time of 72 h, an IC_{50} value higher than 40 μM for diosmin on A549 cell line has previously been reported.[38] The VOdios complex behaved like a slight cytotoxic agent inhibiting about 31% the viability of the lung cancer cells at 100 μM. This result may indicate that the complexation improved the action of the free ligand.

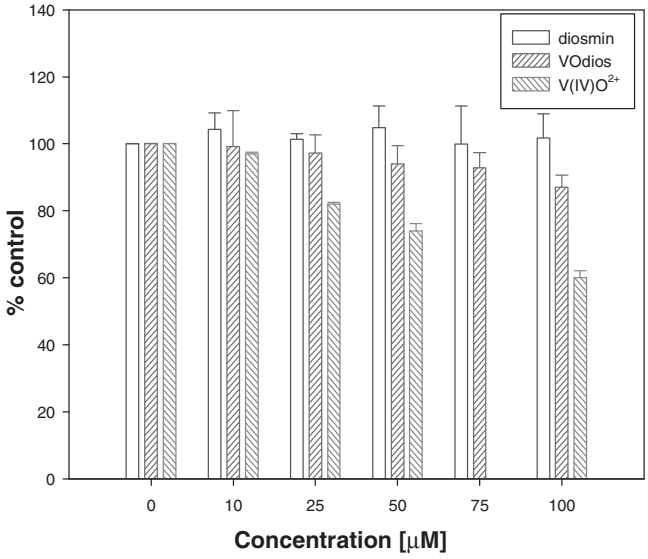

Figure 8. Effect of $V(IV)O^{2+}$ cation, diosmin and VOdios on the extent of deoxyribose degradation by hydroxyl radical. The values are expressed as the mean ± SEM of at least three independent experiments.

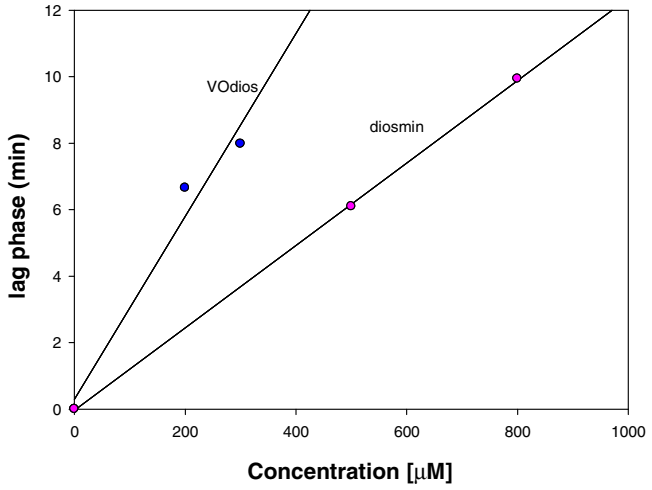

Figure 9. Effect of diosmin and VOdios on AAPH-generated peroxyl radicals pyranine mixture. Changes were calculated as time delay (lag) of pyranine consumption, 37 °C, measured at 454 nm.

Reactive oxygen species (ROS) are partially reduced derivates of molecular oxygen which have been considered as cytotoxic products of cellular metabolism and their accumulation in cells may promote cell death. DHR123 is the reduced form of rhodamine and is unreactive towards $O_2^{\cdot-}$ and H_2O_2 in the absence of catalysts. Fluorescent Rhodamine 123 is directly formed in the presence of $OH^{\cdot}$, $CO_3^{\cdot-}$, $NO_2^{\cdot}$, HClO, $ONNO^-$ and Fe^{+2}. In this respect, DHR123 constitutes a marker of overall oxidant levels.[43] As shown in Figure 11 VOdios treatment induced an increase in ROS levels (ca. 200% at 100 μM). On the other hand, the ROS levels are similar to those of the cancer cell line (control) in the presence of diosmin and oxidovanadium(IV) cation. These results agree with the respective effects observed in the viability assay.

From the examination of A549 cells morphology after 10 and 100 μM VOdios treatment, 24 h incubation (Fig. 12), it was observed that the cells began to show symptoms of the cell death. An increase in cytoplasm condensation, loss of connections between cells and pycnotic nuclei can be observed.

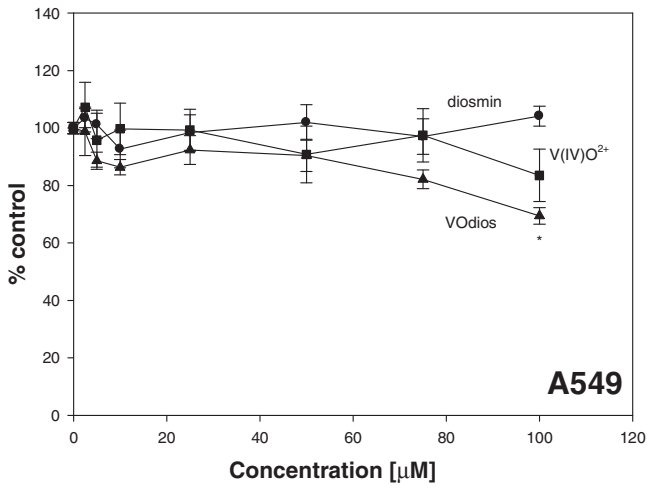

Figure 10. Inhibitory effects of diosmin (circles), VOdios (triangles) and oxidovanadium(IV) cation (squares) on A549 cell viability. The cell line was treated with various concentrations of the compounds for 24 h. The results are expressed as the percentage of the basal level and represent the mean ± the standard error of the mean (SEM) from three separate experiments. *Significant values in comparison with the control level (P <0.05).

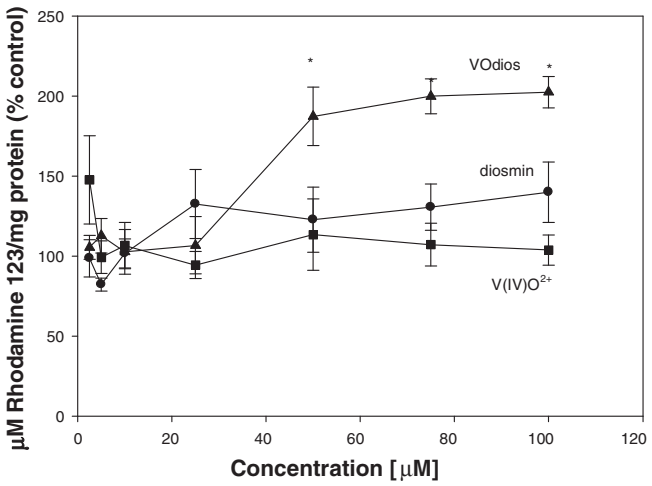

Figure 11. Effect of diosmin, VOdios and oxidovanadium(IV) cation on dihydrorhodamine 123 (DHR123) oxidation to rhodamine 123. A549 cells were incubated at 37 °C in the presence of 10 µM DHR123. The values are expressed as a percentage of the control level for DHR123 oxidation to rhodamine 123 and represent the mean ± SEM. *Significant values in comparison with the control level (P <0.05).

3.4.3. Breast cancer

The effect of diosmin, VOdios and oxidovanadium(IV) cation on the viability of human breast cancer cell lines (T47D, SKBR3 and MDAMB231) was examined by the MTT assay (Fig. 13). The free ligand did not display an antiproliferative behavior on the SKBR3 cell line and on the T47D cell line it exhibited and IC_{50} value higher than 100 µM. This latter result is in agreement with previous reported data on other breast cancer cell line, MCF-7.[44] On the other hand, diosmin inhibited the MDAMB231 cell viability (IC_{50} ca. 70 µM). The oxidovanadium(IV) complex, VOdios, behaved as a strong cytotoxic agent with IC_{50} values of 23.3 µM, 46.4 µM and 11.6 µM (on T47D, SKBR3 and MDAMB231 cell viability), respectively. Comparing these values with those obtained for the oxidovanadium(IV) cation (>100, 92.1 and 45.4 µM) and for diosmin, it can be determined that the anti-cancer effects of the flavonoid has been improved by metal complexation.

3.4.4. Mechanisms of action

According to the mechanistic determinations (Table 3) the cytotoxic effects of the oxidovanadium(IV) cation in these breast cancer cell lines were not related to the mitochondrial apoptotic pathway. This behavior has previously been shown for the MDA-MB231,[45] T47D[21] and SKBr3[22] cell lines. The loss of the mitochondrial membrane potential is related to the initial events that initiate the apoptotic processes. From Table 3 we can conclude that the cytotoxic effect of the compounds on the three cell lines was exerted without mitochondrial membrane damage. Moreover, caspase activation is characteristic for the apoptotic process. The behavior of the three compounds could be related to a caspase 3/7 independent mechanism because no caspase activation was detected. It can be concluded that a caspase-independent form of cell death may play a role for the anticancer response of the flavonoid, the oxidovanadium(IV) cation and their coordination complex.

Oxidative stress plays an important role as a mediator of apoptotic cell death via both the mitochondria-dependent and mitochondria-independent pathways.[46] The mitochondria-dependent pathway has been discarded because of the absence of the membrane damage. Given that the tested compounds did not produce appreciable changes in the cellular ROS production at 24 h incubation (Table 3) an oxidative stress mechanism was ruled out. The mechanism of cell death can be divided into passive (massive damage) or active (the cell itself contributes to its own death). Apoptosis is the best-characterized form of programmed cell death and requires the activation of caspase proteases to bring about rapid cell death that displays distinctive morphological and biochemical hallmarks. Non-apoptotic cell death, such as necroptosis, autophagic cell death, pyroptosis and caspase-independent cell death occurs independently of apoptosis.[47] Considering the results of the mechanistic studies shown in Table 3, a non-apoptotic form of cell death in a caspase- and oxidative stress-independent manner for the anticancer effect of the tested compounds could be suggested.

3.4.5. Bovine serum albumin (BSA) interactions

The studies concerning the interaction and potential transport with bovine serum albumin were made with diosmin and the VOdios complex measuring the florescence intensity of BSA before and after addition of these compounds. The interaction with oxidovanadium cation was previously discussed.[22] It has been demonstrated that the increment of concentrations of $V(IV)O^{2+}$ barely changed the fluorescence intensity of BSA leading to a 10% quenching at the higher tested concentration values.

As depicted in Figure 14A and B, BSA showed strong fluorescence emission while diosmin and VOdios showed no intrinsic fluorescence at the measured range of wavelengths. The fluorescence intensity decreased with increasing the concentrations of the added compounds (fluorescence quenching). Usually, the modifications in the fluorescence emission spectra of BSA are indicative of the changes around the microenvironment of Trp residue. A blue shift of the emission peak is related to the exposition of the amino acid residue Trp to a more hydrophobic environment while a red shift indicated that microenvironment of Trp residue turned to be more hydrophilic.[48] From Figure 14 it can be observed a red spectral shift upon the interaction of the compounds with BSA suggesting that microenvironment of tryptophan residue turned to be more hydrophilic.

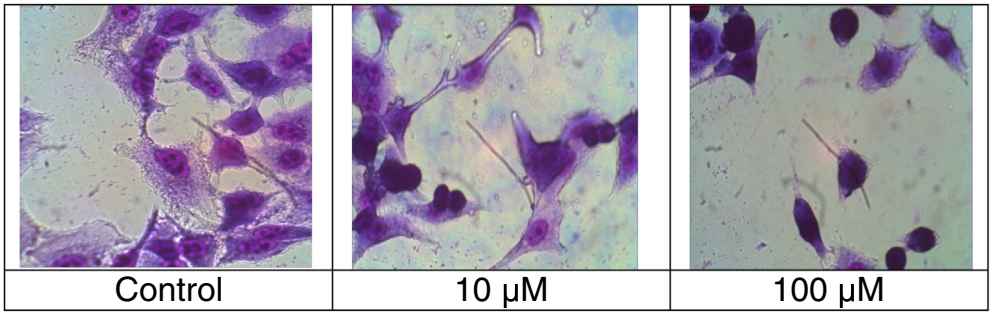

Figure 12. Effect of the treatment of A549 cell line with VOdios on cell morphology. Cells were incubated for 24 h without drug addition (control) and with VOdios (10 and 100 µM, 40×).

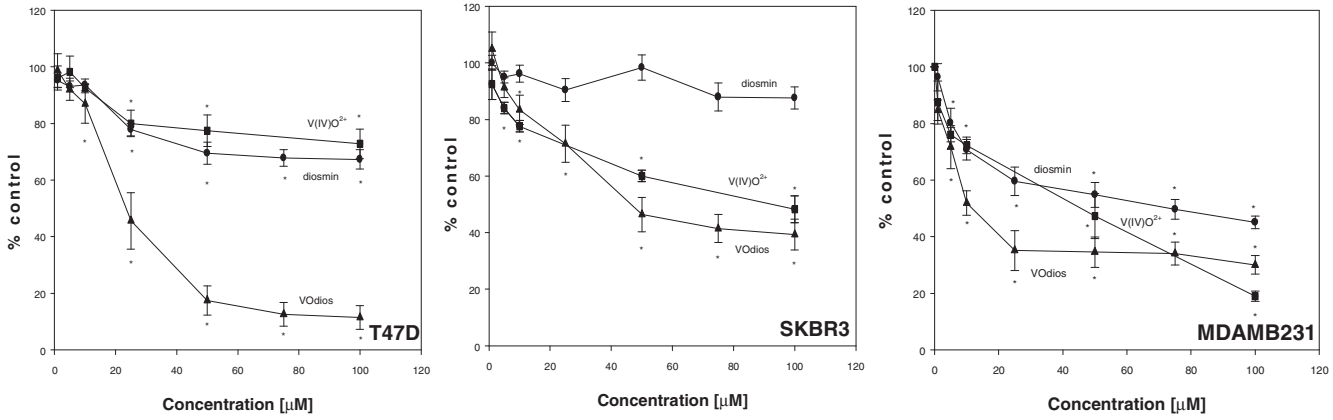

Figure 13. Inhibitory effects of diosmin (circles), VOdios (triangles) and oxidovanadium(IV) cation (squares) on cell viability of human breast cancer cell lines (T47D, SKBR3 and MDAMB231). All cell lines were treated with different concentrations of the compounds for 24 h. The results are expressed as the percentage of the control level and represent the mean ± the standard error of the mean (SEM) from three separate experiments. *Significant values in comparison with the control level (P <0.05).

Table 3
High content cytotoxicity assay. Effects of 10 μM diosmin, VOdios and oxidovanadium(IV) cation at 24 h incubation on T47D, SKBR3 and MDAMB231 cell lines on ROS production, disruption of the mitochondrial membrane potential (TMRM) and caspases 3/7 activation. Results are expressed as the percentage of the measured control level and represent the mean values ± the standard error of the mean (SEM) from three separate experiments. Control: untreated cells

	T47D			SKBR3			MDAMB231		
	ROS	TMRM	Caspases 3/7 Activation	ROS	TMRM	Caspases 3/7 Activation	ROS	TMRM	Caspases 3/7 Activation
Diosmin	105 ± 7	96 ± 7	99 ± 9	104 ± 2	78 ± 8	116 ± 2	110 ± 7	104 ± 3	106 ± 17
VOdios	106 ± 9	105 ± 8	90 ± 9	103 ± 2	97 ± 6	112 ± 13	107 ± 2	110 ± 9	122 ± 5
$V(IV)O^{2+}$	123 ± 10	100 ± 1	101 ± 17	101 ± 8	96 ± 4	101 ± 0	98 ± 3	109 ± 6	115 ± 17

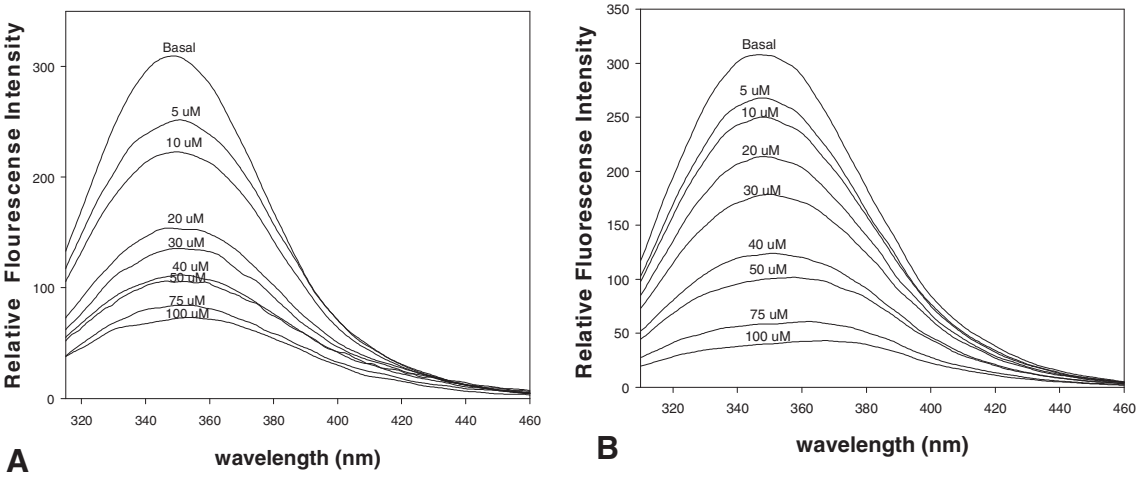

Figure 14. The fluorescence spectra of BSA (6 μM) at different concentrations of diosmin (A) and VOdios (B). λ_{ex} = 280 nm, T = 298 K.

To confirm the quenching mechanism, the fluorescence data have been analyzed at different temperatures with the well-known Stern–Volmer (1) equation.

$$F_0/F = 1 + K_q\tau_0[Q] = 1 + K_{SV}[Q] \quad (1)$$

where F_0 and F are the fluorescence intensities in the absence and presence of quencher, respectively; K_q is the bimolecular quenching constant; τ_0 is the lifetime of the fluorophore in the absence of quencher, and Q is the concentration of quencher. As shown in Figure 15A, the Stern–Volmer plot for diosmin is linear, which indicates that only one type of quenching occurs. This static quenching is often observed if the fluorophore can have a stacking interaction with the quencher, if the latter have aromatic rings, like diosmin. The K_{sv} values (Table 4) resulted similar to those obtained for the interaction of diosmin with human serum albumin (HSA) and the same mechanism of static quenching is then proposed in this case taken into consideration the decrease of K_{sv} with the increase of the temperature.[29]

Within certain concentrations, the curve of F_0/F versus [Q] would be linear if the quenching type is single static or dynamic quenching. If the quenching type is combined quenching (both static and dynamic), the Stern–Volmer plot is an upward curvature. Positive deviations from the Stern–Volmer equation are frequently observed when the extent of quenching is large. This is the case of the quenching of tryptophan fluorescence in proteins by polar or charged quenchers that do not penetrate the hydrophobic interior of proteins, and only those tryptophan residues on the surface of the protein are quenched.[49]

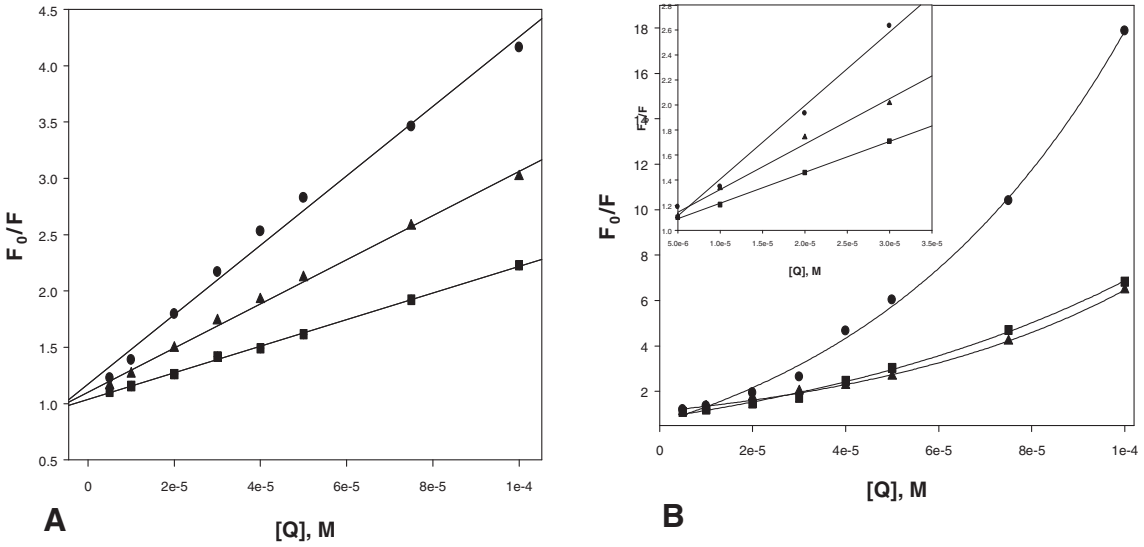

Figure 15. Plots of F_0/F versus [Q] for BSA with diosmin (A) and VOdios (B) at different temperatures ((●), 298 K; (▲), 303 K; (■), 310 K), λ_{ex} = 280 nm.

Table 4
Stern–Volmer constant (K_{sv}), quenching rate constant (K_q), binding constant (K_a) and n binding sites for the interaction of diosmin and VOdios with BSA (6 μM) in Tris–HCl buffer (0.1 M, pH 7.4)

Compounds	T (K)	K_{sv} ($\times 10^4$) (L mol^{-1})	r^2	K_q ($\times 10^{12}$) (L mol^{-1} s^{-1})	K_a ($\times 10^4$)(L mol^{-1})	n
Diosmin	298	3.08 ± 0.07	0.9915	3.08 ± 0.07	1.84 ± 0.32	0.93 ± 0.02
	303	1.95 ± 0.06	0.9966	1.95 ± 0.06	0.88 ± 0.15	0.89 ± 0.01
	310	1.18 ± 0.01	0.9986	1.18 ± 0.01	0.19 ± 0.08	0.84 ± 0.03
VOdios	298	5.10 ± 0.02	0.9840	5.10 ± 0.02	55.3 ± 0.07	1.22 ± 0.001
	303	3.63 ± 0.02	0.9887	3.63 ± 0.02	46.3 ± 0.15	1.24 ± 0.01
	310	2.46 ± 0.02	0.9989	2.46 ± 0.02	5.17 ± 0.2	1.06 ± 0.01

The complex VOdios showed upward-curving Stern–Volmer plots (Fig. 15B). Nevertheless, it could be shown that at low concentrations, the curves were linear indicating a single quenching (static or dynamic quenching). A linear correlation was obtained at concentrations up to 30 μM and the calculated K_{sv} value resulted 5.10×10^4 (25 °C) (Table 4). This value is too large to be due to collisional quenching. Considering that the value of K_q (where $K_{sv} = K_q \tau_0$ and $\tau_0 = 10^{-8}$ s)[48] resulted in the order of 10^{12} M^{-1} s^{-1} (Table 4), a value higher than the maximum diffusion limited rate (10^{10} M^{-1} s^{-1}), both tested compounds must be bound to the BSA.[48]

The binding constant (K_a) of the interaction of small molecules bounded to a set of equivalent sites on a macromolecule and the number of binding sites (n), can be calculated plotting log $[(F_0 - F)/F]$ versus log[Q][48] (Eq. 2 and Fig. 16)

$$\log[(F_0 - F)/F] = \log K_a + n \log[Q] \quad (2)$$

The binding affinity of diosmin (Table 4) resulted smaller than that of naringenin and luteolin,[22,26] measured under the same experimental conditions ($K_a = 1.84 \times 10^4$ M^{-1}, 10.20×10^4 M^{-1} and 65.10×10^6 M^{-1}, respectively). It has to be mentioned that the neutral form of diosmin predominated at physiological pH values. This lower value of binding constant can be explained by structural-binding affinity relationships which showed that glycosylation of the flavonoid produced steric hindrance in the binding pocket that weakened the binding affinity and increases the polarity of the molecule lessening the ability of the flavonoid to penetrate into the tryptophan-rich hydrophobic interior regions of BSA.[50] From Table 4 it can be seen that the binding of VOdios with BSA is stronger than that of the flavonoid maybe due to anionic character of the complex. The number of binding sites between the compounds and BSA, approximately equal to 1, indicated that there is only one binding site in the BSA molecule.

To determine the interaction of the compounds with BSA, the thermodynamic parameters were calculated from the temperature dependence of the binding constants for the BSA-compound binding (van't Hoff plots)

$$\ln K_a = -\Delta H^0/RT + \Delta S^0/R \quad (3)$$

where R is the gas constant, T is the experimental temperature, and K_a is the binding constant at corresponding T. The free energy change (ΔG^0) is then estimated from the following equation:

$$\Delta G^0 = \Delta H^0 - T\Delta S^0 \quad (4)$$

For both compounds negative $\Delta S°$ values have been obtained (Table 5) evidencing the presence of van der Waals forces. The negative value of $\Delta H°$ suggested that the binding processes were predominately enthalpy driven and hydrogen bonding favored the interactions. This postulation is based on the conceptual model of protein association proposed by Ross et al.[51] that give the expected signs of contributions to the ΔH and ΔS values taking into account the penetration of hydration layers producing a disorder of the solvent and the interactions in the short-range. Therefore, both hydrogen bond and van der Waals forces played a major role in the binding of diosmin and VOdios to BSA, and at higher temperatures dissociation of weakly bound complexes resulted. Spontaneity of the interaction process was evident from the negative $\Delta G°$ values.

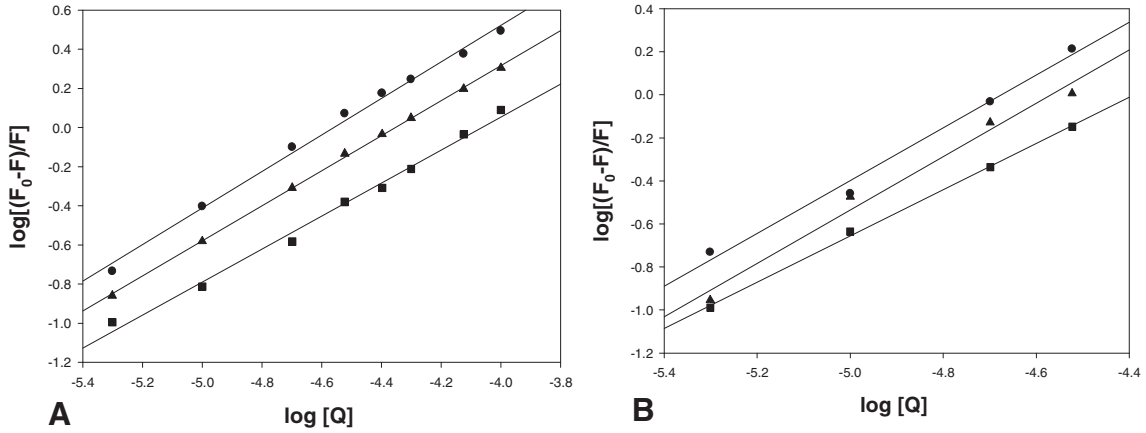

Figure 16. Plots of $\log(F^0 - F)/F$ versus $\log[Q]$ for BSA with diosmin (A) and VOdios (B) at different temperatures: (●) 298 K; (▲) 303 K; (■) 310 K, λ_{ex} = 280 nm.

Table 5
Thermodynamic parameters for the interaction of BSA with diosmin and VOdios at different temperatures

Compounds	ΔH^0 (kJ/mol)	ΔS^0 (J/mol)	ΔG^0 (kJ/mol)
Diosmin	−146.68	−490.91	−24.53 (298 K) −22.48 (303 K) −19.61 (310 K)
VOdios	−156.81	−413.67	−33.73 (298 K) −31.67 (303 K) −28.78 (310 K)

4. Conclusion

A new oxidovanadium(IV) cation with the flavonoid diosmin has been synthesized and characterized. The main structural feature of this complex is that the coordination to the ligand occurred through the deprotonated hydroxyl sugars of the rutinoside moiety of diosmin. Among the tested free radicals this structural modification produced a slight improvement of the diosmin antioxidant action only against peroxyl radicals. Because the coordination did not occur through the flavonoid moiety of the ligand an electron delocalization from V=O to the aromatic ring to stabilize the flavonoid radical produced by the interaction with the free radicals, is precluded. Besides, diosmin behaved as a poor effective like anticancer agent on all the tested cell lines but the complexation improved the cell-killing capacity of VOdios. An oxidative stress mechanism of action has been established for VOdios on the lung cancer cell lines. Although the complex behaved as a more effective agent against the breast cancer cell lines, a caspase-independent mechanism has been evidenced for its cell-killing action because it did not produce caspase 3/7 activation, mitochondrial membrane damage or cellular ROS generation. The same mechanistic behavior has been found for both the ligand and the metal cation. Diosmin, in its neutral ionization form and concentrations ranging from 0.5 to 100 μM binds with BSA to form a 1:1 compound protein, by a static quenching process. This binding allowed the transport and storage of the drugs in the bodies. The affinity of the flavonoid by BSA is smaller than that of other flavonoids because of the glycosidic bond that produces steric hindrance to penetrate into the tryptophan-rich hydrophobic interior regions of BSA. The binding affinity has been improved by complexation of the flavonoid with the oxidovanadium(IV) cation, with higher contributions to the hydrogen bond and van der Waals forces, may be because of the anionic nature of the metal complex. In summary, both compounds can be stored and distributed by BSA in the biological systems.

Acknowledgements

This work was supported by UNLP, CONICET, CICPBA (PICyT 813/13) and ANPCyT (PICT-2013-0569), Argentina. V.R.M. is a fellowship holder from ANPCyT. E.G.F., L.G.N. are research fellows of CONICET. P.A.M.W. is a research fellow of CICPBA, Argentina. Convenio de vinculación tecnológica. Expte-CONICET-004200/13; TQ1/13.

References and notes

1. Jiang, N.; Jin, L.; Teixeira da Silva, J. A.; Islam, Z.; Gao, H.; Liu, Y.; Peng, S. *Sci. Hortic.* **2014**, *168*, 73.
2. Díaz, L.; Del Río, J. A.; Perez-Gilabert, M.; Ortuno, A. *Plant Physiol. Biochem.* **2015**, *89*, 11.
3. *Flavonoids: Chemistry, Biochemistry, and Applications*; Andersen, Ø. M., Markham, K. R., Eds.; CRC Press Taylor & Francis Group: Boca Raton, 2006.
4. Silambarasan, T.; Raja, B. *Eur. J. Pharmacol.* **2012**, *679*, 81.
5. Bunaciu, A. A.; Udristioiu, G. E.; Ruţă, L. L.; Fleschin, Ş.; Aboul-Enein, H. Y. *Saudi Pharm. J.* **2009**, *17*, 303.
6. Ramelet, A. A. *Angiology* **2001**, *51*, S49.
7. Etcheverry, S. B.; Ferrer, E. G.; Naso, L.; Rivadeneira, J.; Salinas, V.; Williams, P. A. M. *J. Biol. Inorg. Chem.* **2008**, *13*, 435.
8. Onishi, M. *Photometric Determination of Traces of Metals, Chemical Analysis*, 4th ed.; Wiley: NewYork, 1989.
9. Kuo, C. C.; Shih, M.; Kuo, Y.; Chiang, W. *J. Agric. Food Chem.* **2001**, *49*, 1564.
10. Yamaguchi, T.; Takamura, H.; Matoba, T. C.; Terao, J. *Biosci. Biotechnol. Biochem.* **1998**, *62*, 1201.
11. Halliwell, B.; Gutteridge, J. M. C.; Aruoma, O. *Anal. Biochem.* **1987**, *165*, 215.
12. Huang, W. Y.; Majumder, K.; Wu, J. *Food Chem.* **2010**, *23*, 635.
13. Hapner, C. D.; Deuster, P.; Chen, Y. *Chem. Biol. Interact.* **2010**, *186*, 275.
14. Bradford, M. *Anal. Biochem.* **1976**, *72*, 248.
15. Ai, F.; Ma, Y.; Wang, J.; Li, Y. *Iran. J. Pharm. Res.* **2014**, *13*, 1115.
16. Gopalakrishnan, V.; Pillai, S. I.; Subramanian, S. P. *Biochem. Res. Int.* **2015**, *1*, 2015.
17. Aghel, N.; Ramezani, Z.; Beiranvand, S. *Pakistan J. Biol. Sci.* **2008**, *11*, 2451.
18. Ferrer, E. G.; Salinas, M. V.; Correa, M. J.; Naso, L.; Barrio, D. A.; Etcheverry, S. B.; Lezama, L.; Rojo, T.; Williams, P. A. M. *J. Biol. Inorg. Chem.* **2006**, *11*, 791.
19. Naso, L.; Ferrer, E. G.; Lezama, L.; Rojo, T.; Etcheverry, S. B.; Williams, P. A. M. *J. Biol. Inorg. Chem.* **2010**, *15*, 889.
20. Naso, L. G.; Ferrer, E. G.; Butenko, N.; Cavaco, I.; Lezama, L.; Rojo, T.; Etcheverry, S. B.; Williams, P. A. M. *J. Biol. Inorg. Chem.* **2011**, *16*, 653.
21. Naso, L. G.; Lezama, L.; Rojo, T.; Etcheverry, S. B.; Valcarcel, M.; Roura-Ferrer, M.; Salado, C.; Ferrer, E. G.; Williams, P. A. M. *Chem. Biol. Interact.* **2013**, *206*, 289.
22. Islas, M. S.; Naso, L. G.; Lezama, L.; Valcarcel, M.; Salado, C.; Roura-Ferrer, M.; Ferrer, E. G.; Williams, P. A. M. *J. Inorg. Biochem.* **2015**, *149*, 12.
23. Etcheverry, S. B.; Williams, P. A. M.; Baran, E. J. *Carbohydr. Res.* **1997**, *302*, 131.
24. Etcheverry, S. B.; Barrio, D. A.; Williams, P. A. M.; Baran, E. J. *Biol. Trace Elem. Res.* **2001**, *84*, 227.
25. Williams, P. A. M.; Etcheverry, S. B.; Baran, E. J. *Carbohydr. Res.* **2000**, *329*, 41.
26. Naso, L. G.; Lezama, L.; Valcarcel, M.; Salado, C.; Villacé, P.; Kortazar, D.; Ferrer, E. G.; Williams, P. A. M. *J. Inorg. Biochem.* **2016**, *157*, 80.
27. Chasteen, N. D. Vanadyl (IV) Spin Probes, Inorganic and Biochemical Aspects In *Biological magnetic resonance*; Berliner, L. J., Reuben, J., Eds.; Plenum: New York, 1981; Vol. 3..
28. Smith, T. S., II; LoBrutto, R.; Pecoraro, V. L. *Coord. Chem. Rev.* **2002**, *228*, 1.

29. Barreca, D.; Laganà, G.; Bruno, G.; Magazù, S.; Bellocco, E. *Biochimie* **2013**, *95*, 2042.
30. Satterfield, M.; Brodbelt, J. S. *Anal. Chem.* **2000**, *72*, 5898.
31. Rice-Evans, C. A.; Miller, N. J.; Paganga, G. *Free Radical Biol. Med.* **1996**, *20*, 933.
32. Cypriani, B.; Limasset, B.; Carrié, M.; Le Doucen, C.; Roussie, M.; de Paulet, A. C.; Damon, M. *Biochem. Pharmacol.* **1993**, *45*, 1531.
33. Senthamizhselvan, O.; Manivannan, J.; Silambarasan, T.; Raja, B. *Eur. J. Pharmacol.* **2014**, *736*, 131.
34. Khlebnikov, A. I.; Schepetkin, I. A.; Domina, N. G.; Kirpotinab, L. N.; Quinn, M. T. *Bioorg. Med. Chem.* **2007**, *15*, 1749.
35. Sroka, Z.; Fecka, I.; Cisowski, W. *Z. Naturforsch.* **2005**, *60c*, 826.
36. Wang, N.; Yang, X. W. *J. Asian Nat. Prod. Res.* **2010**, *12*, 1044.
37. Mir, S. A.; Bhat, A. S.; Ahangar, A. A. *Int. J. Pharm. Tech. Res.* **2014**, *6*, 759.
38. KawaII, S.; Tomono, Y.; Katase, E.; Ogawa, K.; Yano, M. *Biosci. Biotechnol. Biochem.* **1999**, *63*, 896.
39. Manthey, J.; Guthrie, N. *J. Agric. Food Chem.* **2002**, *50*, 5837.
40. López-Lázaro, M.; Galvez, M.; Martín-Cordero, C.; Ayuso, M. J. *Stud. Nat. Prod. Chem.* **2002**, *27*, 891.
41. Dung, T. D.; Day, C. H.; Binh, T. V.; Lin, C.; Hsu, H.; Su, C.; Lin, Y.; Tsai, F.; Kuo, W.; Chen, L.; Huang, C. *Food Chem. Toxicol.* **2012**, *50*, 1802.
42. Martínez, C.; Vicente, V.; Yáñez, J.; Alcaraz, M.; Castells, M. T.; Canteras, M.; Benavente-García, O.; Castillo, J. *Histol. Histopathol.* **2005**, *20*, 1121.
43. Forkink, M.; Smeitink, J. A. M.; Roland Brock, P. H. G.; Willems, M.; Koopman, W. J. H. *Biochim. Biophys. Acta* **2010**, *1797*, 1034.
44. Ciolino, H. P.; Wang, T. T. Y.; Yeh, G. C. *Cancer Res.* **1998**, *58*, 2754.
45. Naso, L.; Valcarcel, M.; Villacé, P.; Roura-Ferrer, M.; Salado, C.; Ferrer, E. G.; Williams, P. A. M. *New J. Chem.* **2014**, *38*, 2414.
46. Sinha, K.; Das, J.; Pal, P. B.; Sil, P. C. *Arch. Toxicol.* **2013**, *87*, 1157.
47. Tait, S. W. G.; Ichim, G.; Green, D. R. *J. Cell Sci.* **2014**, *127*, 2135.
48. Tang, L.; Jia, W. *Spectrochim. Acta, Part A: Mol. Biomol. Spectrosc.* **2013**, *103*, 114.
49. Lakowicz, J. R. *Principles of Fluorescence Spectroscopy*, 3rd ed.; Springer: New York, 2006.
50. Liu, E. H.; Qi, L. W.; Li, P. *Molecules* **2010**, *15*, 9092.
51. Ross, P. D.; Subramanian, S. *Biochemistry* **1981**, *20*, 3096.